

Article

Raman Spectroscopy Application in Food Waste Analysis: A Step towards a Portable Food Quality-Warning System

Omar Hussein Dib ¹, Ali Assaf ^{1,*}, Alexia Pean ¹, Marie-Jose Durand ¹, Sullivan Jouanneau ¹, Ramakrishnan Ramanathan ²  and Gérald Thouand ¹

¹ Nantes Université, ONIRIS, CNRS, GEPEA, UMR 6144, F-85000 La Roche-sur-Yon, France

² Essex Business School, Southend Campus, Elmer Approach, Southend-on-Sea SS1 1LW, UK

* Correspondence: ali.assaf1@univ-nantes.fr

Abstract: Food waste is one of the main problems contributing to climate change, as its piling up in landfills produces the greenhouse gas methane. Food waste occurs at every stage of food production; however, a major source of food waste occurs at businesses that supply food to consumers. Industry 4.0 technologies have shown promise in helping to reduce food waste in food supply chains. However, more innovative technologies, such as Raman spectroscopy, hold great promise in helping to reduce food waste, although this has largely been ignored in the literature. In this context, we propose a portable Raman platform to monitor food quality during transportation. The developed system was tested in conditions mimicking those present in a refrigerated truck by analyzing chicken samples stored at temperatures of 4 °C. Raman spectra were acquired for non-packaged and packaged samples over the duration of 30 days resulting in 6000 spectra. The analysis of Raman spectra revealed that the system was able to detect noticeable changes in chicken quality starting on day six. The main Raman bands contributing to this change are amide I and tyrosine. The proposed system will offer the potential to reduce food losses during transportation by consistently checking the food quality over time.

Keywords: food waste; Raman spectroscopy; food quality; protein



Citation: Dib, O.H.; Assaf, A.; Pean, A.; Durand, M.-J.; Jouanneau, S.; Ramanathan, R.; Thouand, G. Raman Spectroscopy Application in Food Waste Analysis: A Step towards a Portable Food Quality-Warning System. *Sustainability* **2023**, *15*, 188. <https://doi.org/10.3390/su15010188>

Academic Editor: Flavio Boccia

Received: 29 November 2022

Revised: 16 December 2022

Accepted: 17 December 2022

Published: 22 December 2022



Copyright: © 2022 by the authors. Licensee MDPI, Basel, Switzerland. This article is an open access article distributed under the terms and conditions of the Creative Commons Attribution (CC BY) license (<https://creativecommons.org/licenses/by/4.0/>).

1. Introduction

The estimated global food waste recorded by the United Nations Environment Programme in 2021 was about 931 million tons [1]. The causes of food waste are abundant and occur from farm to fork, i.e., during production, processing, distribution and selling, and lastly, consumption. Furthermore, the increasing concerns around climate change, land use, water use and loss of biodiversity have encouraged researchers and scientists to come up with new rapid and accurate methods to assess food quality and prevent food waste along the production–consumption chain.

Traditionally, evaluating food quality is done using a direct approach, particularly by conducting a microbial analysis. This analysis is necessary for determining the shelf life and quality loss of a food product [2]. Since microbial load and microflora composition are quite important parameters for detecting food quality, such analysis is impossible to execute at certain stages of the food and marketing chain, such as during transportation. Other alternatives would be the use of indirect approaches such as Industry 4.0 technologies which are already being used to help reduce food waste in food supply chains [3]. These technologies generally help monitor storage conditions such as temperature, humidity, light, and vibration, with the help of Internet of Things sensors (IoT). These sensors measure the required parameters and send them to the cloud for remote monitoring. In case the monitoring detects unacceptable storage conditions, then rapid corrective actions are taken (e.g., checking the temperature control mechanisms) in order to guarantee the freshness of food. While these IoT sensors are useful, they do not capture the freshness of food directly,

but rather via related parameters such as temperature or humidity. Instead, there are more innovative technologies, such as Raman spectroscopy, that analyze food directly and are able to measure the freshness of the food more directly.

In recent years, Raman spectroscopy advancements have opened new research insight by allowing rapid and non-destructive analysis. This optical method, which relies on the inelastic scattering of light, is used in several domains of applications: medical, pharmaceutical, food, and microbial detection [4–7]. The main objective of Raman spectroscopy is to simplify the analysis process and to reduce the investigation time of samples. This untargeted screening of food samples aims to evaluate the characteristics of a given product (by the production of a structural fingerprint revealing almost all chemical components, including nucleic acids, carbohydrates, lipids, and proteins) and to relate its spectral fingerprints to distinctive traits such as nutritive value, adulteration, or quality of food. Among spectroscopic methods, Raman and Surface Enhanced Raman Scattering (SERS) are considered promising techniques for food analysis. Both offer a rapid, nondestructive and label-free analysis. The difference between the two methods is that SERS has higher sensitivity allowing the structural detection of low-concentration substances which are difficult to detect using traditional Raman Spectroscopy [8,9]. SERS higher sensitivity is obtained by using an enhancing substrate such as gold (Au), silver (Ag), or copper (Cu). However, the use of such substrate in determining the quality of a food product can complicate the analysis step, especially if the food is packaged. Such a factor makes traditional Raman Spectroscopy preferable over SERS.

Traditional or native Raman Spectroscopy is considered a promising candidate for monitoring food quality, especially meat products. For instance, this type of spectroscopy is capable of studying modifications at the level of secondary protein structures such as amide I ($1650\text{--}1680\text{ cm}^{-1}$), and amide II ($1262\text{--}1313\text{ cm}^{-1}$) regions, as well as C-C groups ($940\text{--}1070\text{ cm}^{-1}$), C-H groups ($1440\text{--}1457\text{ cm}^{-1}$), and amino acids (640 and 850 cm^{-1}) [10,11]. Also, Raman spectroscopy is widely being used in the determination of meat organoleptic properties [12], spoilage [13], pH [14], identification of meat from different animal species [15,16], and studying meat quality from different slaughter animals including chicken [11,17,18]. All the latter studies show that Raman equipment monitoring meat quality is fairly well developed for laboratory testing. Nowadays, and thanks to the technological advancement of Raman, a trend is being noted worldwide towards the promotion of automated quality control [19]. For instance, portable Raman systems have been developed to be used in the meat industry [20]. Moreover, Bauer et al. [21] and Fowler et al. [22] used portable Raman spectrometers to study the tenderness and sensory characteristics of beef. In spite of the latter, their use remains timid in food applications, especially in the reduction of food waste. In addition, the literature on food waste has largely ignored the use of such highly innovative technology so far.

The primary contribution of this paper is to showcase the use of Raman spectroscopy for fighting food waste. The main limitation of applying Raman spectroscopy is the huge size of the equipment, which makes it practically impossible to use this technology in trucks. However, the team of authors has pioneered the development of a portable version of Raman spectroscopy. This is another huge contribution of this paper. We showcase the use of a portable Raman, placed and tested in a refrigerated chamber to mimic the conditions present in a refrigerated truck transporting chicken product from one outlet to another.

2. Materials and Methods

2.1. Sample

About 30 packed cooked boneless chicken breasts with the same production and expiry date were purchased from a local store. The samples were packed under a modified atmosphere ($\text{O}_2 = 68\%$, $\text{CO}_2 = 26\%$ and $\text{N}_2 = 6\%$). After purchasing, the packages were stored directly in a fridge at $4\text{ }^\circ\text{C}$. The samples were then distributed in two stages.

Stage I is considered as a proof of concept, where the sole purpose of this stage is to check which Raman bands are responsible for the shift in chicken quality. In this stage, the chicken breast was removed from the package each day for 30 days and its Raman spectra were measured.

Stage II is the validation stage; this stage was necessary to prove that the proposed Raman system can still check the quality of the chicken through the package (made from low-density polyethylene, LDPE), and to determine on which day there was a noticeable change in the chicken's quality. In this stage, only one of the packed samples was utilized, and the chicken breast wrapped in LDPE was measured directly by Raman spectroscopy for 30 days. About 13 zones were carefully chosen and studied on the surface of the wrapped sample (Figure S1), and the zone with the most informative region was selected for executing stage II.

Stages I and II were done in refrigerated conditions at 4 °C and the spectral measurements were done directly on both surfaces without any pre-treatment (such as fat removal, washing, or mincing).

2.2. Raman System and Measurement

An automatic portable Raman system was used in this study (Figure 1). This system consists of a QE Pro-Raman spectrometer (Ocean Optics, Netherlands) having a dynamic range of 85,000:1 and System SNR: 1000:1 with typical back-thinned CCD array miniature spectrometers cooling to -40 °C below ambient air; Laser source of 785 nm excitation wavelength (Oxxius, France); InPhotonics RPB785 fiber-optic probe consisting of two single fibers (105 μm excitation fiber and a 200- μm collection fiber) with filtering and steering micro-optics contained in a polyurethane jacket; Motorized 3-axis (X, Y, Z) platform (Standa, Opton Laser International, France) with a sample holder; Dark enclosure specifically made to prevent light from interfering with the fiber-optic probe head (numeric aperture: 0.22); Computer running OceanView software (Ocean Optics, Netherlands), and Libximc cross-platform library to control the motorized stage. The whole system was placed in a cold chamber at 4 °C for 30 days.

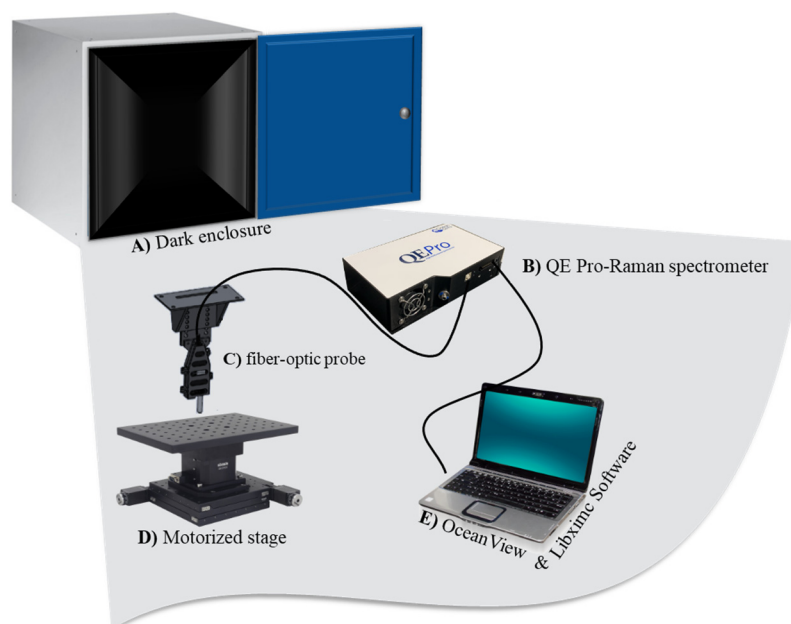


Figure 1. A dark enclosure (A) including the automated Raman system parts: (B) QE Pro-Raman spectrometer, (C) InPhotonics RPB785 fiber-optic probe, (D) Motorized 3-axis (X, Y, Z) platform, and (E) computer running OceanView software and Libximc.

Raman spectra were then collected using the following parameters: laser power of 250 mW, a focal distance of 2 mm with an integration time of 5 s. The spectral resolution

was 5 cm^{-1} in the measured wavelength range of $200\text{--}4000\text{ cm}^{-1}$. The dark spectrum subtraction was performed during each spectral acquisition. For each stage, 100 spectra were collected per day, with the help of the motorized stage, with a total of 3000 spectra over 30 days. The temperature of the chamber was taken two times per day over 30 days to ensure that the temperature did not rise above $4\text{ }^{\circ}\text{C}$.

2.3. Spectra Pre-Processing

Raman spectra were processed using Opus software (Bruker optics GmbH, V 7.2, Germany) and MATLAB software (version R2019b, MathWorks Inc, Natick, MA, USA). The raw data, of a spectral range of $200\text{--}4000\text{ cm}^{-1}$, was first cut in the spectral zone of $500\text{--}3000\text{ cm}^{-1}$. Then, all cosmic spikes presented in the defined spectral range ($500\text{--}3000\text{ cm}^{-1}$) were manually eliminated before applying data treatment. All spectra were then baseline corrected using an elastic concave method (64° and ten iterations), smoothed based on the Savitzky-Golay algorithm, and lastly normalized using min–max normalization.

2.4. Data Analysis

After spectral processing, the treated spectra were subjected to multivariate data analysis, specifically, Principal Component Analysis (PCA). PCA is a technique commonly used to transform large datasets into two smaller sets, referred to as the score matrix and the loading matrix. This orthogonal transformation allows the observation of trends and clusters, and uncovers the relationship between observations and variables by plotting the principal components (PCs) and the loading plots [23]. Accordingly, the number of PC components to be used was determined using a scree plot. PCs were represented by scatter plots and the correlation among the variables can be inspected through loading plots.

PC scores (PC1 score of stage II) were subjected to Kruskal Wallis (KW) test. This test is a non-parametric test and is used to compare samples from three or more groups of independent observations [24]. It was selected to establish statistical significance ($p\text{-value} < 0.05$), and also because it is more stable to outliers. PCA and KW were computed using the SAISIR Package [25]. All statistical analysis was performed using MATLAB software (version R2019b, MathWorks Inc, Natick, MA, USA).

3. Results and Discussion

The portable Raman system was tested in two stages to confirm its ability to monitor the quality of chicken over 30 days. These tests are essential in order to verify that the Raman sensor can give reliable results under any circumstances before launching it in the field. The main obstacle confronted was the introduction of a package layer between the probe (laser) and the sample (chicken breast).

3.1. Detecting Changes in Chicken Quality (without Packaging) by Raman Spectroscopy

The first stage of testing included the study of chicken fillet quality with respect to time (30 days) and temperature ($4\text{ }^{\circ}\text{C}$). At this stage, Raman spectra were obtained directly on chicken (without packaging). Before analyzing the data acquired by the Raman sensor, Table 1 illustrates the various molecular vibrations present naturally in the chicken breast Raman spectrum [10]. For instance, the familiar Amide I bands, with their different configurations (α -helix and β -helix) presented at different Raman shifts, as well as amide III representing collagen at 1313 cm^{-1} , the C-H bending at 1440 cm^{-1} , and C-C stretch at $2906\text{--}3011\text{ cm}^{-1}$. Additionally, other Raman bands can be observed when analyzing chicken meat that corresponds to aromatic amino acids such as phenylalanine at 1077 cm^{-1} , and tyrosine (Tyr) at 850 and 640 cm^{-1} . Vibrations from the nucleobase adenine (Ade) and S-S stretching can also be present. All of the latter stated bands, particularly those representing proteins, are the main contributors to the textual characteristics and functional properties of chicken meat, and they will help in highlighting the effect of storage on chicken quality [10,26].

Table 1. Familiar Raman bands present in chicken breast.

Raman Shift (cm ⁻¹)	Vibrational Mode
3011, 2914, 2895, 2854	C-H stretching
1658–1645	Amide I (α -helix)
1680–1665, 1640–1610	Amide I (β -helix)
1665–1660	Amide I (random coil)
1690–1680	Amide I (β -turn)
1457–1440	C-H bending
1313 and 1260	Amide III (collagen)
1240	Amide III (β -sheet and random coil)
1070	C-C stretching (phenylalanine)
850 and 640	Tyrosine stretching-ring
750	Adenine stretching-ring
525	S-S stretching vibration

Other proteins, such as myoglobin or in particular the heme pigments of myoglobin, present in chicken or any other kind of meat can weaken the Raman signal by causing a common phenomenon faced in Raman analysis known as fluorescence background [13]. To acquire the best spectrum, as presented in Figure 2, the fluorescence background was omitted by using a baseline correction algorithm.

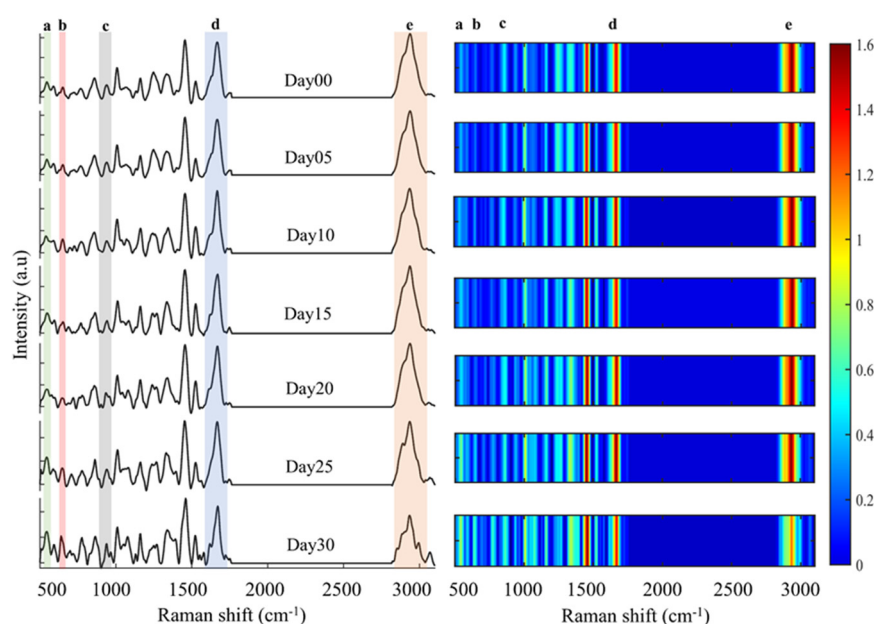


Figure 2. The variation in Raman spectra of chicken breast without packaging over 30 days of storage at 4 °C. The highlighted regions (a–e) represent the vibrational bonds that are changing in function of time. (a): S-S stretching, (b,c): Tyrosine, (d): Amide I (α -helix), (e): C-H stretching.

After spectral treatment, the average spectrum of each five days was taken and plotted. Figure 2 shows the changes detected in chicken Raman spectra over 30 days at 4 °C. Raman spectra obtained on Day 00 were considered as the standard or fresh samples and all other days were compared to it. Of all the Raman bands present in Table 1, five peaks were visually identified that seem to be changing with storage time, as shown in Figure 2. In addition, a pattern regarding the intensities of these peaks was noticed where S-S stretching (a) and Tyrosine (b and c) intensities increased, while those of Amide I (d) and C-H stretching (e) decreased as storage duration increased.

Although Raman signals are gradually changing, as shown in Figure 2, visual goings-over of these changes remain difficult. To have more information on the Raman spectrum changes caused by storage time, PCA multivariate statistical tool was applied to the Raman

spectra (Figure 3). The first, second, and third principal components, or PC1, PC2, and PC3, carried the most spectral variances over 30 days. PC1 explained 30% of the variance, PC2 explained 25% of the variance, and PC3 explained the least with 5%. All other PCs contained less than 1% of the variance between samples. Figure 3 shows the PCA plot of the PC1, PC2 and PC3 scores and their loadings. The PCA plot reveals a separation of the samples based on their quality over time. PC1 clearly distinguishes the spectra of chicken obtained from the 25th to 30th day. This group (days 25 to 30) is separated from the other samples by having a positive sign with respect to PC1. This separation is also clearly observed on PC3 (see Figure S2) where the same group of samples (days 25 to 30) is distinguished from the other samples by having a positive sign on PC3. The main contributions for PC1 and PC3 were from the Tyr band (845 and 640 cm^{-1}) and S-S stretching vibrations (525 cm^{-1}), correlating with a positive sign of loadings (Figure 3B), and from the phenylalanine (1077 cm^{-1}), amide III (1311 cm^{-1}), amide I (1655 cm^{-1}) and C-H stretching (2906 cm^{-1}), correlating with a negative sign of loadings (Figure 3B). Based on the PCA results, the shift in quality in the last five days observed in Figure 3A is due to the decrease in the intensity of all correlated bands with the amide I band, and an increase in the intensity of anti-correlated bands such as Tyr. This increase is a result of the extra amino acids which were formed during storage due to microbial growth and autolysis of meat. Additionally, the decrease in the intensity of Amide I and III (also supported by PC2 scores and loadings) modes or the denaturation of protein is known to occur during storage [10,11,27]. Furthermore, a decrease in the intensity of the band at 1448 cm^{-1} assigned to the CH_2 and CH_3 bending vibration was observed. The latter decrease can be the result of the hydrophobic interactions occurring around the aliphatic residues [10,28]. The results also show an increase in the S-S stretching vibrations (525 cm^{-1}) as recorded by PC1 loadings, which can be attributed to the oxidation of cysteine and methionine amino acid residues [29].

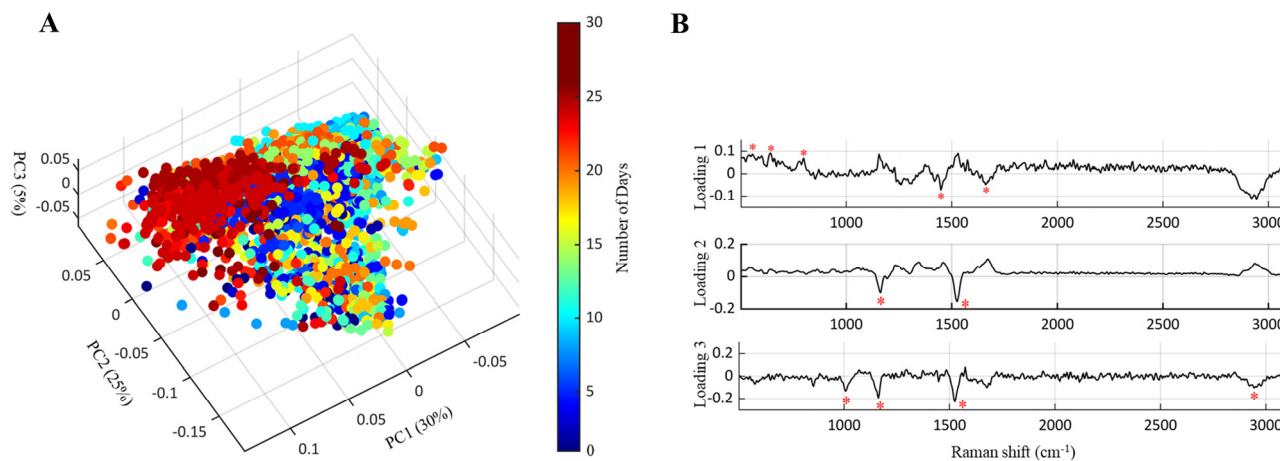


Figure 3. PCA scores (A) and loadings (B) of chicken breast—Quality overview over 30 days of refrigerated storage ($4\text{ }^{\circ}\text{C}$). (A) The scores of the chicken breast spectra of the last ten days (day 21 to day 30) are clearly distinguished from the rest of days where (B) the loading plots show the molecules (represented by a red asterisk) impacted during the testing period.

3.2. Application of Raman Spectroscopy, Dealing with Packaged Food

The second stage of testing involved checking the quality of the LDPE-wrapped chicken breast over 30 days. As is known, LDPE has its unique spectrum [30,31], and its Raman bands can be confused with those of chicken bands, as shown in Figure 4. The LDPE spectrum was therefore acquired and compared with the chicken spectrum (Figure 4). Only a few chicken-related bands were visible (Figure 4), which are Amide I (1655 cm^{-1}) and Tyr (845 and 640 cm^{-1}).

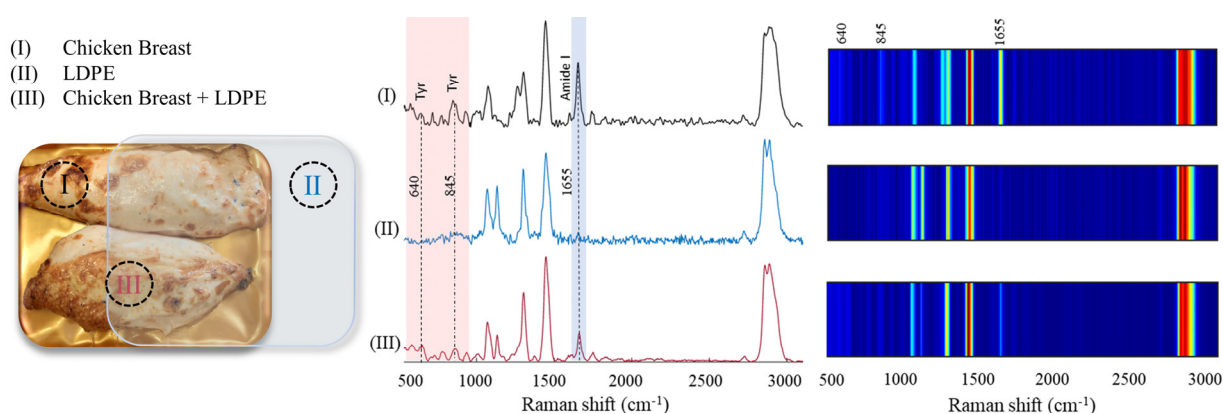


Figure 4. Inspecting the Raman bands of chicken that have no interference with the packaging layer (LDPE). The highlighted regions show two distinct bands: Amide I 1655 cm^{-1} , and Tyrosine (640 and 845 cm^{-1}). (I): Chicken spectra; (II): LDPE spectra; (III): Combined spectra of chicken and LDPE.

Since Amide I and Tyr were the only bands that did not have any interference with LDPE Raman bands, as shown in Figure 4, the effect of these bands on chicken quality was further examined by calculating the area under the curve and correlating the obtained results with PCA scores and loadings. The amide I band is considered an indicator of the total protein concentration [10,11]. Figure 5 shows an inverse relationship between the storage time of chicken fillets and the area under the curve of 1655 cm^{-1} (Amide I). In contrast, Tyr showed a complementary response to storage time, where the peak area increased with time. Additionally, when comparing the first five days of storage with the last five days of storage, there appears to be around a 60% difference in the intensities of both peaks, as shown in Figure 5. We believe that denaturation of Amide I results in the formation of free amino acids, of which Tyr is one of the amino acids detected by Raman spectroscopy. These results are also consistent with those presented previously (Stage I), especially when referring to Amide I and Tyr bands. PCA was also conducted on the Raman data of the LDPE-wrapped chicken breast. Figure 6 shows that PC1 carried the most spectral variances over 30 days, explaining about 87% of the variance. Other PCs (PC2 and PC3) contained about 1% of the variance between samples. PC1 scores show a pattern shifting from left to right, as shown in Figure 6A. It seems that the days with the highest quality (day 00–day 05) have positive scores, shifting towards negative scores until the last five days where the deterioration in quality is the highest. The main contributions for PC1 were from Tyr at 845 and 640 cm^{-1} with a negative sign of loadings, and Amide III and C-H stretching at 1655 cm^{-1} with a positive sign of loadings (Figure 6B). Loadings 2 and 3 did not provide any significant information, as the PC2 and PC3 scores showed negligible variations among the samples.

After establishing the Raman bands responsible for the variation in the quality of chicken wrapped in LDPE, PC1 scores were then subjected to Kruskal Wallis to get an estimate on the day the quality started shifting, and the results are shown in Figure 7A,B. The results show the days on which the portable Raman system was able to detect a change in the chicken's quality. For instance, the first shift in quality was detected on day six, as seen in Figure 7A, where this day seems to separate the samples into two groups as shown in Figure 7B (p -value < 0.05). The same occurs on day 12. However, the biggest shift in PC1 scores was noted after day 21 (Figure 7A), and these results are in accordance with those presented in Figure 5. The total area of Amide I started decreasing from day six, with its highest decrease being recorded on the 30th day.

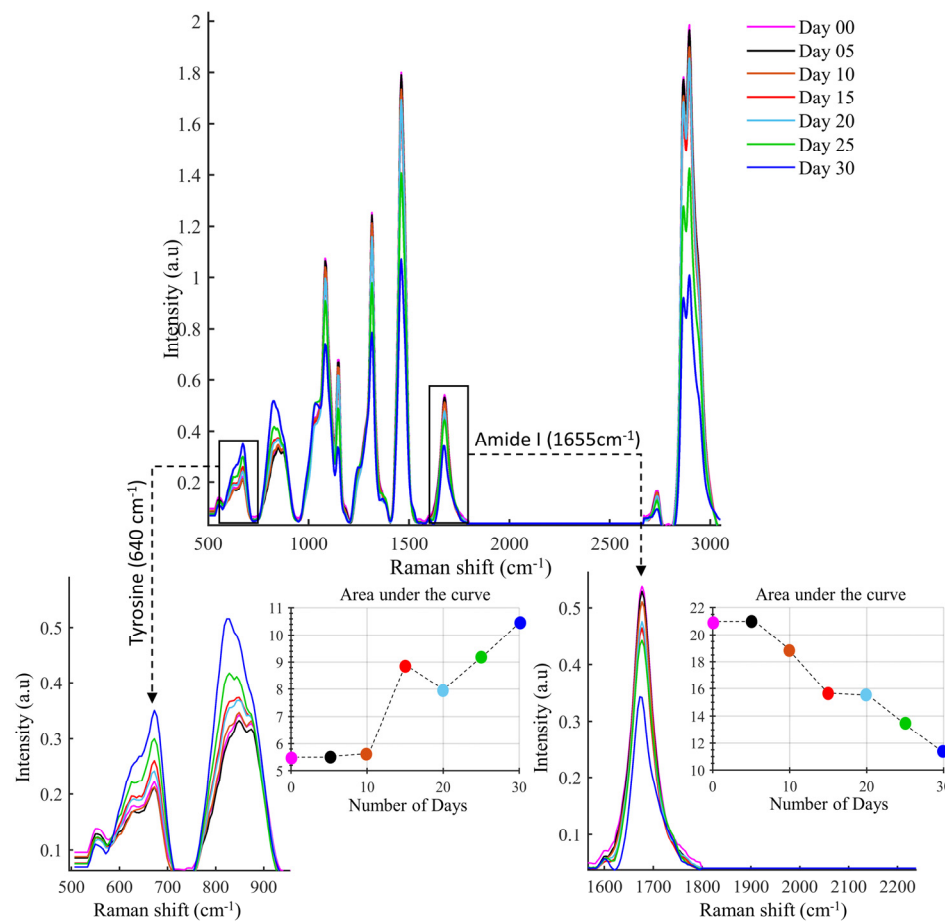


Figure 5. Relation between storage time, intensity and area under the curve of the Raman bands (1655 and 640 cm⁻¹) that had no interference with LDPE. Amide I (1655 cm⁻¹) witnessed a decrease in the intensity and in the area under the curve, whereas Tyrosine (640 cm⁻¹) showed a contrary response as the storage period increased.

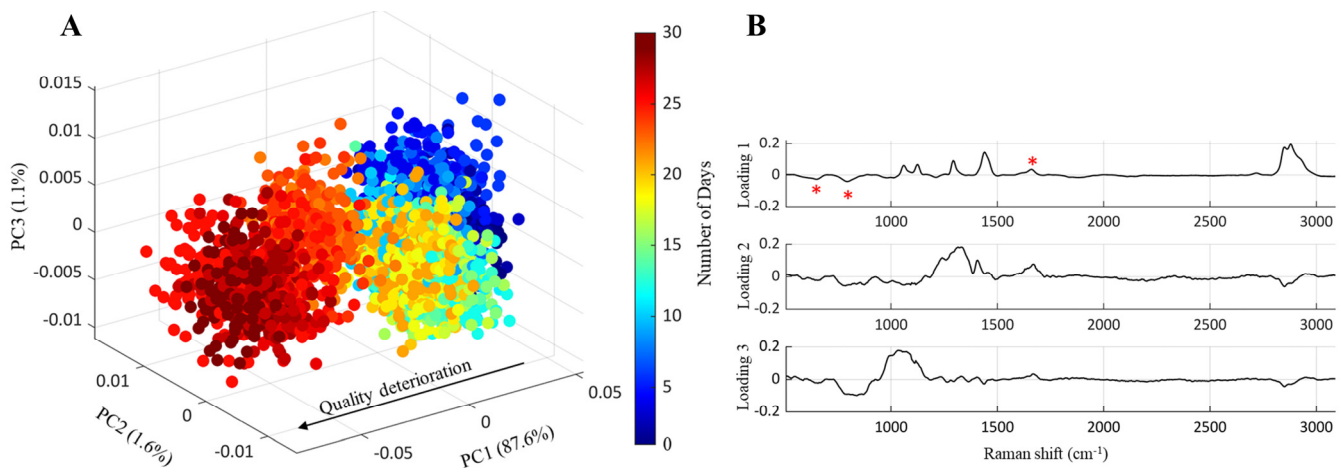


Figure 6. PCA scores (A) and loadings (B) of LDPE-wrapped chicken breast. Quality overview over 30 days of storage at 4 °C. (A) The PC1 scores of the chicken spectra shifted from positive scores (Day 00) toward negative scores (Day 30) as an indicator of quality deterioration. (B) shows the molecules impacted (represented by the red asterisk) during deterioration of the chicken quality, especially on loading 1.

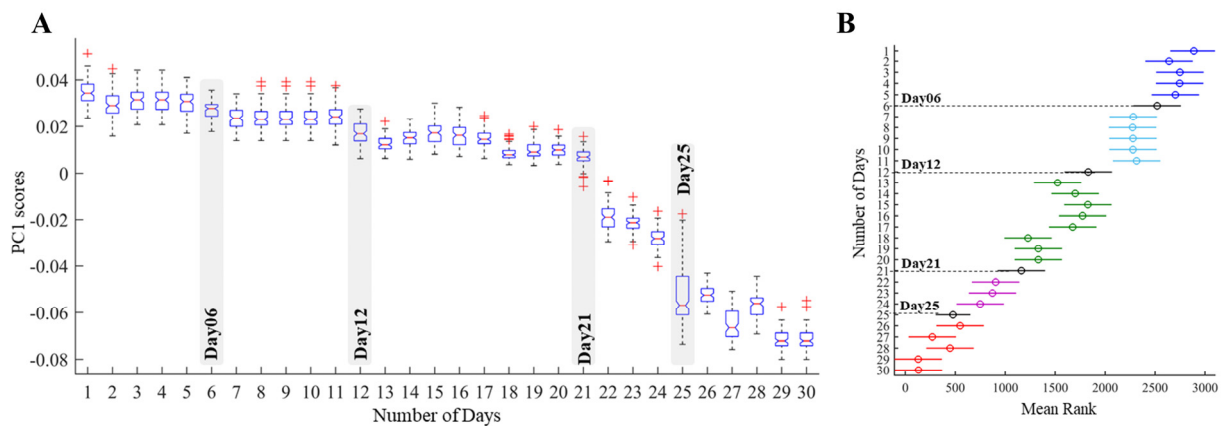


Figure 7. Spotting the days where a shift in the chicken quality is detected by the portable Raman spectroscopy. (A) a box plot representing the median of the PC1 scores per day, where the highlighted region shows the day when a shift in quality is detected. (B) represents the significant groups separated by the dotted black line. This black line represents the day on which the chicken quality has similarity with the groups before and after.

Based on the results obtained during stage I and stage II, it is evident that Raman spectroscopy can monitor the quality of chicken as it spoils. The results of stage I show the change in protein structure as storage time is increased. For instance, amide I and amide III vibrational intensities decreased, while those of Tyr and S-S stretching increased. These changes in the protein structure indicate that there are several spoilage reactions happening, including microbial growth, denaturation of protein, and oxidation of amino acid residues. Additionally, hydrophobic interaction around the aliphatic residues was noticed through the decrease of the CH₂ and CH₃ intensities.

As for stage II, we can observe that the portable Raman spectroscopy was able to monitor the quality of LDPE-wrapped chicken breast. Even though only two peaks were visible when the product was packaged, Amide I is considered one of the primary protein indicators and, through its denaturation, it is possible to monitor the quality of chicken wrapped in LDPE [10,11]. Most importantly, the system was capable of early detection on the day that the shift in quality started.

The provided results can not only help food industries to monitor product quality but also protect the environment. We believe that showcasing the portable version of the Raman spectrometer holds huge promise in our fight against food waste. This can occur in multiple ways along the food production and distribution chain. For instance, monitoring raw materials at the farm level in real-time using the provided system is quite important, as this can provide farmers with valuable information on the chemical composition of raw materials. This permits farmers to better optimize farm management and to cut foreseeable food losses. This is also achievable at the factory level, where the ability of this portable system to detect changes at the molecular level in seconds can pick up any drastic quality changes in any food item (vegetables, fruits, and meats) and thus rush its production. As for transportation, the portable version of the Raman spectrometer can act as an alert system that can signal the driver to deliver the food products to the nearest food outlet or distribution center in case of a possible food loss. However, for this portable system to be considered as an online application, further investigation and analysis—including sensory testing and examination of the microbes—are required to determine if food products can truly have their shelf life predicted by this method.

3.3. Conclusions

Through the chemometric analysis of Raman spectra, collected by a portable fiber-optic Raman spectrometer, it is possible to monitor the quality of packaged chicken meat in the function of storage time. This system was able to detect the shift in the product's

quality, the chemical components impacted during the course of quality deterioration, and the day when the food quality started changing. The capabilities of such a system render it an important contributor to reducing food waste, and its potential is limitless. This is why our future work will focus on increasing the number of tested samples, the use of different food samples, and finally, real-time testing on the road.

Supplementary Materials: The following supporting information can be downloaded at: <https://www.mdpi.com/article/10.3390/su15010188/s1>, Figure S1: Raman spectra were obtained from 13 different zones with the help of a motorized stage; Figure S2: PC3 scores and loadings—Quality overview over 30 days of refrigerated storage (4 °C).

Author Contributions: Conceptualization, G.T. and A.A.; methodology, A.A. and O.H.D.; validation, G.T., A.A., O.H.D., A.P., M.-J.D., S.J. and R.R.; writing—original draft preparation O.H.D.; lab analysis, O.H.D. and A.P.; writing—review and editing, G.T., A.A., O.H.D., A.P., M.-J.D., S.J. and R.R. All authors have read and agreed to the published version of the manuscript.

Funding: This research reported in this paper is based on the work done in the REAMIT project (www.reamit.eu, accessed on 1 December 2022) funded by the Interreg North-West Europe (ref NWE831).

Institutional Review Board Statement: Not applicable.

Informed Consent Statement: Not applicable.

Data Availability Statement: REAMIT project and case-study videos are available at www.reamit.eu (accessed on 1 December 2022).

Acknowledgments: The authors would like to thank partners of the REAMIT (Improving Resource Efficiency of Agribusiness supply chains by Minimising waste using Big Data and Internet of Things sensors) project for their contributions to completing this work.

Conflicts of Interest: The authors declare no competing financial interest and respect the ethics of references.

References

1. UNEP. Food Waste Index Report. 2021. Available online: <https://www.unep.org/resources/report/unep-food-waste-index-report-2021> (accessed on 30 September 2022).
2. Kreyenschmidt, J.; Ibal, R. Modeling Shelf Life Using Microbial Indicators. In *Shelf Life Assessment of Food*; Nicoli, M.C., Ed.; Taylor and Francis Group: Oxfordshire, UK, 2012; pp. 127–163.
3. REAMIT—Improving Resource Efficiency of Agribusiness Supply Chains by Minimising Waste Using Big Data and Internet of Things Sensors. Available online: <https://www.nweurope.eu/projects/project-search/reamit-improving-resource-efficiency-of-agribusiness-supply-chains-by-minimising-waste-using-big-data-and-internet-of-things-sensors/> (accessed on 22 November 2022).
4. Grosso, R.A.; Walther, A.R.; Brunbech, E.; Sørensen, A.; Schebye, B.; Olsen, K.E.; Qu, H.; Hedgaard, M.A.B.; Arnspang, E.C. Detection of low numbers of bacterial cells in a pharmaceutical drug product using Raman spectroscopy and PLS-DA multivariate analysis. *Analyst* **2022**, *147*, 3593–3603. [[CrossRef](#)] [[PubMed](#)]
5. Li, L.; Cao, X.; Zhang, T.; Wu, Q.; Xiang, P.; Shen, C.; Zou, L.; Li, Q. Recent Developments in Surface-Enhanced Raman Spectroscopy and Its Application in Food Analysis: Alcoholic Beverages as an Example. *Foods* **2022**, *11*, 2165. [[CrossRef](#)] [[PubMed](#)]
6. Liu, K.; Zhao, Q.; Li, B.; Zhao, X. Raman Spectroscopy: A Novel Technology for Gastric Cancer. *Diagnosis. Front. Bioeng. Biotechnol.* **2022**, *10*, 856591. [[CrossRef](#)]
7. Thomsen, B.L.; Christensen, J.B.; Rodenko, O.; Usenov, I.; Grønnemose, R.B.; Andersen, T.E.; Lassen, M. Accurate and fast identification of minimally prepared bacteria phenotypes using Raman spectroscopy assisted by machine learning. *Sci. Rep* **2022**, *12*, 16436. [[CrossRef](#)]
8. Kadam, U.S.; Chavhan, R.L.; Schulz, B.; Irudayaraj, J. Single molecule Raman spectroscopic assay to detect transgene from GM plants. *Anal. Biochem.* **2017**, *532*, 60–63. [[CrossRef](#)]
9. Lee Seunghyun, S. Kadam Ulhas, Craig Ana Paula, Irudayaraj Joseph. In *In Vivo Biodetection Using Surface-Enhanced Raman Spectroscopy*; Jun, L.N.W., Ed.; Taylor and Francis Group: Boca Raton, FL, USA, 2014; p. 22.
10. Herrero, A.M. Raman spectroscopy for monitoring protein structure in muscle food systems. *Crit. Rev. Food Sci. Nutr.* **2008**, *48*, 512–523. [[CrossRef](#)] [[PubMed](#)]
11. Jaafreh, S.; Breuch, R.; Günther, K.; Kreyenschmidt, J.; Kaul, P. Rapid Poultry Spoilage Evaluation Using Portable Fiber-Optic Raman Spectrometer. *Food Anal. Methods* **2018**, *11*, 2320–2328. [[CrossRef](#)]

12. Wang, Q.; Lonergan, S.M.; Yu, C. Rapid determination of pork sensory quality using Raman spectroscopy. *Meat Sci.* **2012**, *91*, 232–239. [[CrossRef](#)]
13. Sowoidnich, K.; Schmidt, H.; Kronfeldt, H.-D.; Schwägele, F. A portable 671nm Raman sensor system for rapid meat spoilage identification. *Vib.Spectrosc* **2012**, *62*, 70. [[CrossRef](#)]
14. Nache, M.; Hinrichs, J.; Scheier, R.; Schmidt, H.; Hitzmann, B. Prediction of the pH as indicator of porcine meat quality using Raman spectroscopy and metaheuristics. *Chemom. Intell. Lab. Syst.* **2016**, *154*, 45–51. [[CrossRef](#)]
15. Boyaci, İ.H.; Uysal, R.S.; Temiz, T.; Shendi, E.G.; Yadegari, R.J.; Rishkan, M.M.; Velioglu, H.M.; Tamer, U.; Ozay, D.S.; Vural, H. A rapid method for determination of the origin of meat and meat products based on the extracted fat spectra by using of Raman spectroscopy and chemometric method. *Eur. Food Res. Technol.* **2014**, *238*, 845–852. [[CrossRef](#)]
16. Saleem, M.; Amin, A.; Irfan, M. Raman spectroscopy based characterization of cow, goat and buffalo fats. *J. Food Sci. Technol.* **2021**, *58*, 234–243. [[CrossRef](#)] [[PubMed](#)]
17. Lyndgaard, L.B.; Sørensen, K.M.; van den Berg, F.; Engelsens, S.B. Depth profiling of porcine adipose tissue by Raman spectroscopy. *J. Raman Spectrosc* **2012**, *43*, 482–489. [[CrossRef](#)]
18. Motoyama, M.; Chikuni, K.; Narita, T.; Aikawa, K.; Sasaki, K. In Situ Raman Spectrometric Analysis of Crystallinity and Crystal Polymorphism of Fat in Porcine Adipose Tissue. *J. Agric. Food. Chem.* **2013**, *61*, 69–75. [[CrossRef](#)] [[PubMed](#)]
19. Shi, Y.; Wang, X.; Borhan, M.S.; Young, J.; Newman, D.; Berg, E.; Sun, X. A Review on Meat Quality Evaluation Methods Based on Non-Destructive Computer Vision and Artificial Intelligence Technologies. *Food Sci. Anim. Resour.* **2021**, *41*, 563–588. [[CrossRef](#)] [[PubMed](#)]
20. Santos, C.C.; Zhao, J.; Dong, X.; Lonergan, S.M.; Huff-Lonergan, E.; Outhouse, A.; Wheeler, T.L. Predicting aged pork quality using a portable Raman device. *Meat Sci.* **2018**, *145*, 79–85. [[CrossRef](#)] [[PubMed](#)]
21. Bauer, A.; Scheier, R.; Eberle, T.; Schmidt, H. Assessment of tenderness of aged bovine gluteus medius muscles using Raman spectroscopy. *Meat Sci.* **2016**, *115*, 27–33. [[CrossRef](#)]
22. Fowler, S.M.; Schmidt, H.; van de Ven, R.; Hopkins, D.L. Preliminary investigation of the use of Raman spectroscopy to predict meat and eating quality traits of beef loins. *Meat Sci.* **2018**, *138*, 53–58. [[CrossRef](#)]
23. Cordella, C. PCA: The Basic building block of chemometrics. In *Analytical Chemistry*; Ira, S.K., Ed.; Intechopen: London, UK, 2012; p. 146.
24. Kruskal, W.H.; Wallis, W.A. Use of Ranks in One-Criterion Variance Analysis. *J. Am.Stat.Assoc.* **1952**, *47*, 583–621. Available online: <http://www.jstor.org/stable/2280779> (accessed on 30 September 2022). [[CrossRef](#)]
25. Cordella, C.B.Y.; Bertrand, D. SAISIR: A New General Chemometric Toolbox. *TrAC* **2014**, *54*, 75–82. [[CrossRef](#)]
26. Ellis, D.I.; Broadhurst, D.; Kell, D.B.; Rowland, J.J.; Goodacre, R. Rapid and quantitative detection of the microbial spoilage of meat by fourier transform infrared spectroscopy and machine learning. *Appl. Environ. Microbiol.* **2002**, *68*, 2822–2888. [[CrossRef](#)] [[PubMed](#)]
27. Zając, A.; Dymińska, L.; Lorenc, J.; Hanuza, J. Fourier Transform Infrared and Raman Spectroscopy Studies of the Time-Dependent Changes in Chicken Meat as a Tool for Recording Spoilage Processes. *Food Anal. Methods.* **2017**, *10*, 640–648. [[CrossRef](#)]
28. Careche, M.; Herrero, A.M.; Rodriguez-Casado, A.; Del Mazo, M.L.; Carmona, P. Structural Changes of Hake (*Merluccius merluccius* L.) Fillets: Effects of Freezing and Frozen Storage. *J. Agric. Food. Chem.* **1999**, *47*, 952–959. [[CrossRef](#)] [[PubMed](#)]
29. Feng, X.; Moon, S.H.; Lee, H.Y.; Ahn, D.U. Effect of irradiation on the parameters that influence quality characteristics of raw turkey breast meat. *Radiat. Phys. Chem.* **2017**, *130*, 40–46. [[CrossRef](#)]
30. Katsara, K.; Kenanakis, G.; Alissandrakis, E.; Papadakis, V.M. Low-Density Polyethylene Migration from Food Packaging on Cured Meat Products Detected by Micro-Raman Spectroscopy. *Microplastics* **2022**, *1*, 428–439. [[CrossRef](#)]
31. Tselios, C.; Bikiaris, D.; Savidis, P.; Panayiotou, C.; Larena, A. Glass-fiber reinforcement of in situ compatibilized polypropylene/polyethylene blends. *J. Mater. Sci.* **1999**, *34*, 385–394. [[CrossRef](#)]

Disclaimer/Publisher’s Note: The statements, opinions and data contained in all publications are solely those of the individual author(s) and contributor(s) and not of MDPI and/or the editor(s). MDPI and/or the editor(s) disclaim responsibility for any injury to people or property resulting from any ideas, methods, instructions or products referred to in the content.